Supporting Information

to

A sodium bis(perfluoropinacol) borate-based electrolyte for stable, high-performance room temperature sodium-sulfur batteries based on sulfurized poly(acrylonitrile)

Table S1. Combustion elemental analysis of Na-PPB.

Element	Calculated (%)	Found (%)
C	24.38	24.21
H	1.279	1.318
C : H	19.062	18.361

Table S2. Combustion elemental analysis of an SPAN cathode.

Element	wt.%				Atomic ratio
	S	C	N	H	C/S
SPAN	40.24	42.36	13.43	0.9883	2.81

Table S3. Comparison of oxidation potentials of the various existing electrolyte system for RT Na-S batteries.

Salt / molar	Solvent	Working electrode	Oxidation potential V (vs. Na^+/Na)
NaTFSI / 2M	PC:FEC (1:1) + 10 mM InI_3	SS	5.2 [1]
NaTFSI / 2M	TMP:FEC (7:3)	SS	4.6 [2]
$NaB(hfip)_4$ / 1M	EC:DMC + FEC (1:1) + 13 wt.%	Pt	4.65 [3]
$NaCF_3SO_3$ / 1M	Triglyme	Carbon-coated Al	4.0 [4]
Na-PPB / 1M	PC + (FEC, 10 wt.%)	Al	>5.5 (This work)

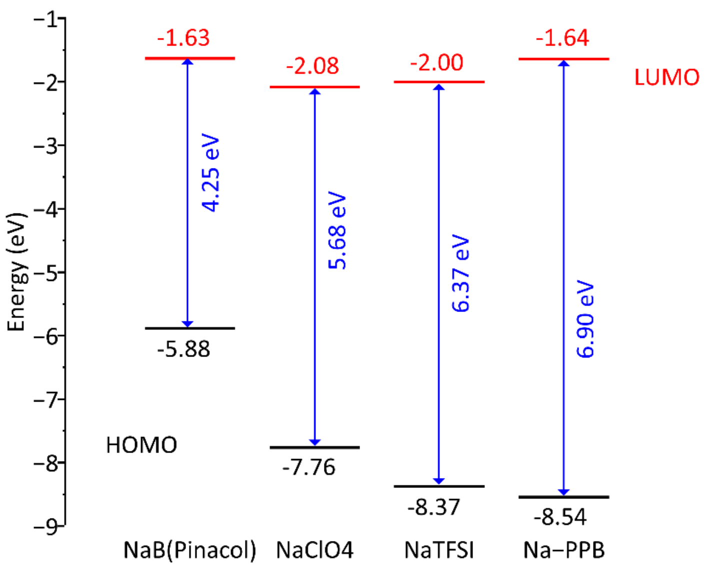

Figure S1. Comparison of HOMO and LUMO energy levels of sodium bis(pinacol) borate, $NaClO_4$, NaTFSI, and Na-PPB.

The calculation of the HOMO and LUMO energy levels was performed with the Gaussian 09 software package using DFT. All energies are calculated at the B3LYP/6-31+G(2d,p) level. We compared the HOMO energy levels of different salts to validate the high oxidation resistance of

Na-PPB. Thus, commercially available salts such as $NaClO_4$ and NaTFSI and a non-fluorinated sodium bis(pinacol) borate HOMO energy levels were calculated and compared with Na-PPB. From Figure S1, it is evident that Na-PPB has a lower HOMO energy level (-8.54 eV) than its counterparts. It is reasonable to associate oxidative stability of the molecule to their HOMO energy level since oxidation results in loosing of an electron from its HOMO. The electron-withdrawing group in the molecule is responsible for lowering the HOMO energy level which in turn increases stability against oxidation. Based on the calculation results, Na-PPB has excellent oxidation stability compared to commercially available sodium salts.

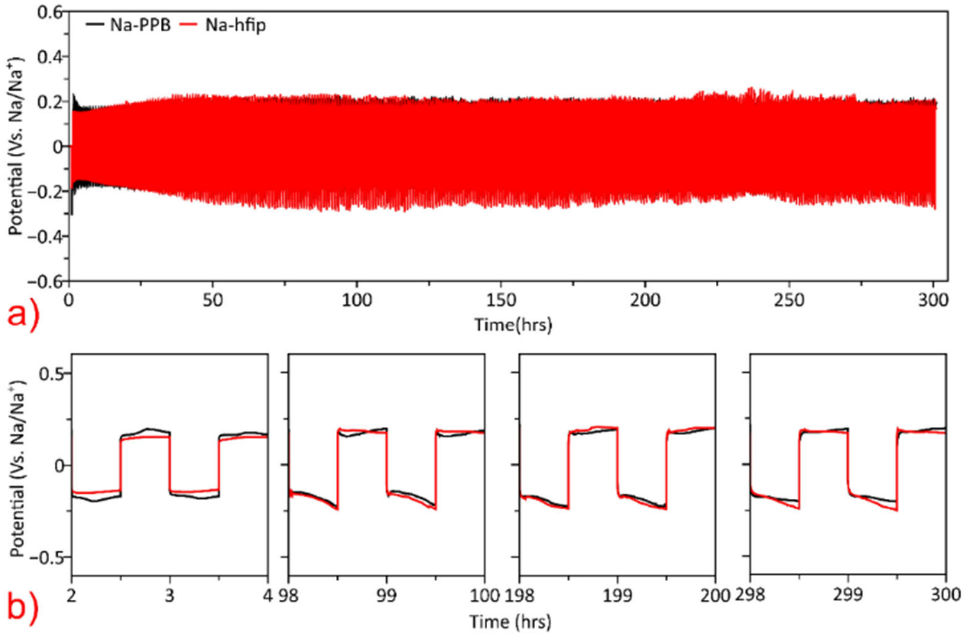

Figure S2. Na||Na symmetrical cell voltage profile at 1 mA cm^{-2} (0.5 mAh cm^{-2}) for Na-PPB and Na-hfip.

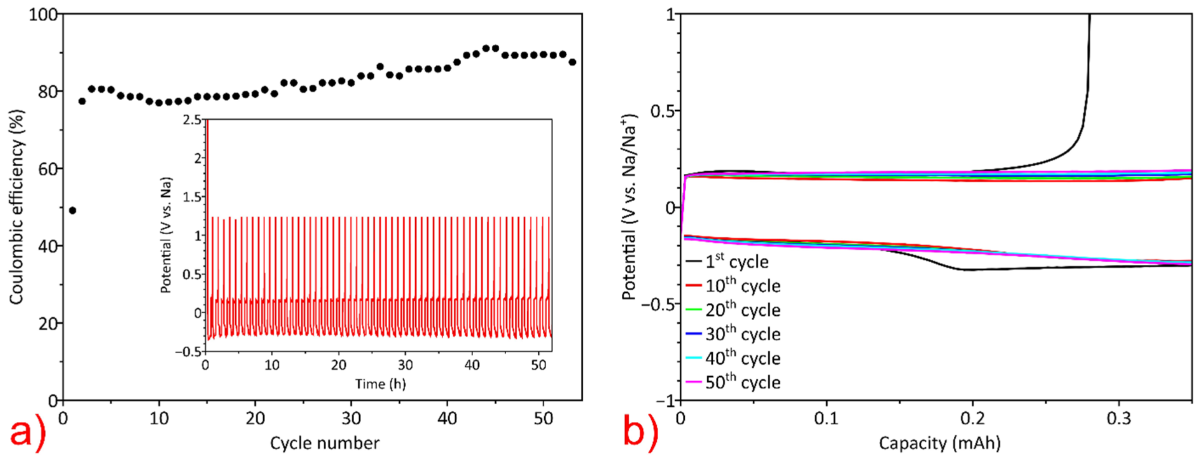

Figure S3. Cycling performance of a Na-PPB electrolyte with graphite as a working electrode, a) coulombic efficiency (inset: chronopotentiogram); b) comparison of voltage versus capacity plot at various cycles.

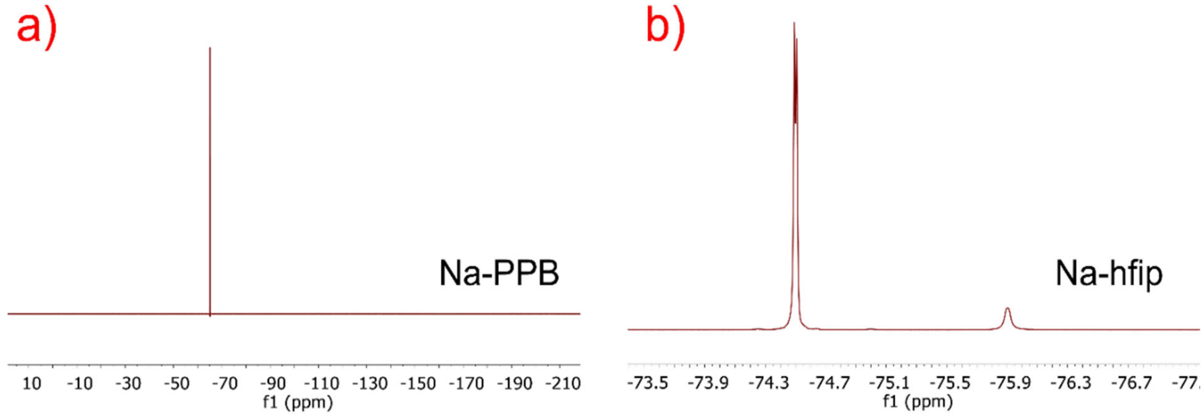

Figure S4. ^{19}F -NMR spectra of a) Na-PPB and b) Na-hfip kept under ambient conditions for 20 days.

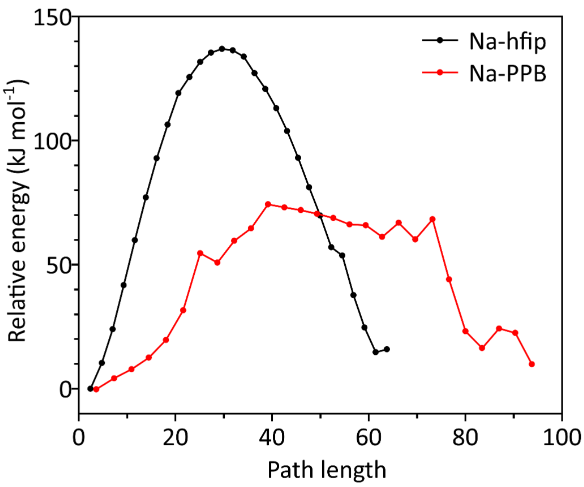

Figure S5. Energy profile along the reaction path (NEB calculations) of both salts, representing the potential barrier between two local minima of the respective salt.

Table S4. Comparison of the morphological changes of Na-hfip and Na-PPB after exposure to air for 20 days.

Samples	Na-hfip	Na-PPB
Pristine		
After exposure to air for 20 days		
Remarks	Color changed to pure white and loss of material	Almost similar to the initial state except for a slight color change

Table S5. Comparison of the weight loss of Na-PPB and Na-hfip after exposure to air for 20 days.

Sample	Initial weight (g)	Weight (g) after 20 days in air	Weight loss (%)
Na-PPB	0.0686	0.0491	28
Na-hfip	0.1347	0.0128	91

Table S6. Comparison of cycling performance of RT Na-S systems with various sulfur-based cathodes.

Cathode system	Electrolyte	C - rate / current	Capacity (mAh g^{-1})	Cycle life	Coulombic efficiency (%)
Electrospun SPAN	0.8 M $NaClO_4$ in EC + DEC (v = 1:1)	1 C	153	500	99.93 [5]
SPAN cathode	1 M $NaClO_4$ in EC + DMC (v = 1 : 1) + 8 wt% FEC	0.5 C	1000	1000	~100 [6]
Selenium-doped SPAN	1 M $NaClO_4$ in PC + PC (v = 1:1)	0.4 A g^{-1}	~770	500	~100 [7]
Tellurium-doped SPAN	1 M $NaClO_4$ in PC + DMC (v = 1:1) + 10 wt% FEC	0.5 A g^{-1}	~970	600	~100 [8]
Iodine-doped SPAN	1 M NaClO4 in EC + DEC (v = 1 : 1) + 8 wt% FEC	2 C	674	500	>99 [9]
S / C composite	1.5 M NaClO4 + 0.3 M $NaNO_3$ in tetraglyme	-	400	20	- [10]
Sulfur in slit micropore	1 M $NaClO_4$ in EC + PC (v = 1 : 1) + 2 wt% FEC	1 C	~640	2000	~100 [11]
SPAN cathode	1 M Na-PPB in PC + 10 wt%FEC	2 C	>950	500	>99.8 (This work)

References

[1] X. Xu, D. Zhou, X. Qin, K. Lin, F. Kang, B. Li, D. Shanmukaraj, T. Rojo, M. Armand, G. Wang, *Nat. Commun.* **2018**, *9*, 3870.

[2] J. Wu, J. Liu, Z. Lu, K. Lin, Y.-Q. Lyu, B. Li, F. Ciucci, J.-K. Kim, *Energy Storage Mater.* **2019**, *23*, 8-16.

[3] S. Murugan, S. Niesen, J. Kappler, K. Küster, U. Starke, M. R. Buchmeiser, *Batter. Supercaps*, https://doi.org/10.1002/batt.202100125.

[4] D. Di Lecce, L. Minnetti, D. Polidoro, V. Marangon, J. Hassoun, *Ionics* **2019**, *25*, 3129-3141.

[5] T. H. Hwang, D. S. Jung, J.-S. Kim, B. G. Kim, J. W. Choi, *Nano Letters* **2013**, *13*, 4532-4538.

[6] A. Y. S. Eng, D.-T. Nguyen, V. Kumar, G. S. Subramanian, M.-F. Ng, Z. W. Seh, *J. Mater. Chem. A* **2020**, *8*, 22983-22997.

[7] L. Wang, X. Chen, S. Li, J. Yang, Y. Sun, L. Peng, B. Shan, J. Xie, *J. Mater. Chem. A* **2019**, *7*, 12732-12739.

[8] S. Li, Z. Zeng, J. Yang, Z. Han, W. Hu, L. Wang, J. Ma, B. Shan, J. Xie, *ACS Appl. Energy Mater.* **2019**, *2*, 2956-2964.

[9] S. Ma, P. Zuo, H. Zhang, Z. Yu, C. Cui, M. He, G. Yin, *ChemComm* **2019**, *55*, 5267-5270.

[10] X. Yu, A. Manthiram, *ChemElectroChem* **2014**, *1*, 1275-1280.

[11] Q. Guo, S. Li, X. Liu, H. Lu, X. Chang, H. Zhang, X. Zhu, Q. Xia, C. Yan, H. Xia, *Adv. Sci.* **2020**, *7*, 1903246.